Sulfate Aerosol Indirect Effect and CO_2 Greenhouse Forcing: Equilibrium Response of the LMD GCM and Associated Cloud Feedbacks

HERVÉ LE TREUT, MICHÈLE FORICHON, OLIVIER BOUCHER, AND ZHAO-XIN LI

Laboratoire de Météorologie Dynamique, CNRS, Paris, France

(Manuscript received 10 September 1996, in final form 21 July 1997)

ABSTRACT

The climate sensitivity to various forcings, and in particular to changes in CO_2 and sulfate aerosol concentrations, imposed separately or in a combined manner, is studied with an atmospheric general circulation model coupled to a simple slab oceanic model. The atmospheric model includes a rather detailed treatment of warm cloud microphysics and takes the aerosol indirect effects into account explicitly, although in a simplified manner. The structure of the model response appears to be organized at a global scale, with a partial independence from the geographical structure of the forcing. Atmospheric and surface feedbacks are likely to explain this feature. In particular the cloud feedbacks play a very similar role in the CO_2 and aerosol experiments, but with opposite sign. These results strengthen the idea, already apparent from other studies, that, in spite of their different nature and their different geographical and vertical distributions, aerosol may have substantially counteracted the climate effect of greenhouse gases, at least in the Northern Hemisphere, during the twentieth century. When the effects of the two forcings are added, the model response is not symmetric between the two hemispheres. This feature is also consistent with the findings of other modeling groups and has implications for the detection of future climate changes.

1. Introduction

The sensitivity of the climate system to perturbations of its radiative equilibrium is largely the consequence of strong feedback processes. These feedbacks are caused by changes in surface albedo, water vapor content, or cloud properties, to name only the most important parameters. In present climate models they generally act as positive feedbacks, which means that they amplify any initial perturbation. These processes strongly control the global sensitivity of the climate in response to given modifications of its boundary conditions. The objective of the present study is to determine to what extent they also constrain the geographical response of the climate system.

For that purpose, we compare the equilibrium response of the model to different prescribed forcings. The nature and amplitude of these forcings refer to the anthropogenic influence over the past century. Two main factors are considered, because they are probably the dominant terms of this past evolution and have very different effects: the CO_2 content or the sulfate aerosol loading. Whereas the CO_2 increase represents a positive climate forcing, inducing a warming, the increased aerosol concentration may have resulted in a negative climate forcing, by increasing reflection of solar radiation, both directly and indirectly through a modification of cloud properties. This effect is not only opposite to the greenhouse warming effect in sign, but also in nature, because it acts on the shortwave component of the radiative balance of the earth, rather than on the longwave component. This implies a different vertical distribution of the radiative perturbation. In addition the geographical distribution of the anthropogenic increase in sulfate aerosol is very specific, with higher concentrations over the Northern Hemisphere continents. In our experiments the anthropogenic CO_2 and sulfate effects happen to have similar magnitudes (although opposite signs). We have used this coincidence to study also the nonlinear effects associated with the combination of different forcings.

As our main objective is to compare the atmospheric feedbacks in response to these forcings, it has been necessary to include first in our model an adequate description of the relevant physical mechanisms. We have used for this purpose an explicit representation of the cloud liquid phase microphysics (Boucher et al. 1995). Our model is the Laboratoire de Météorologie Dynamique (LMD) GCM Cycle 4, coupled to a simple slab ocean. It has already been used for a large number of sensitivity experiments—changes in the solar constant (Nesmes-Ribes et al. 1993), CO_2 doubling (Le Treut et al. 1994), ozone perturbation (Chalita et al. 1996)—to which we will also refer.

Corresponding author address: Dr. Hervé Le Treut, Laboratoire de Météorologie Dynamique du CNRS, casier 99, 4 Place Jussieu, 75252 Paris Cedex 05, France.
E-mail: letreut@lmd.jussieu.fr

The aerosol direct effect consists in aerosol backscattering of visible radiation, thereby increasing the planetary albedo. It is active notably, but not exclusively, in clear-sky situations. Charlson et al. (1987) have shown that an indirect aerosol effect can add up to this direct effect. It is due to the fact that an increase in aerosol concentration can produce an increase in cloud condensation nuclei (CCN), with two potential effects: (i) the condensation of the same amount of water vapor on a larger number of CCN would form a larger number of droplets of smaller size, which would increase the cloud reflectivity; and (ii) droplets of smaller size would also affect the precipitation process, and therefore modify (generally increase) the cloud water content, which in turn increases the cloud optical thickness. The quantification of this indirect effect is even more uncertain than the direct component (Penner et al. 1994; Boucher and Lohmann 1995). These uncertainties in the magnitude (and distribution) of the aerosol direct and indirect forcings may be opposed to the greenhouse gases forcing, which is rather well determined (Cess et al. 1993).

The detailed setting of the model and the experiments are given in sections 2 and 3. The results are discussed in section 4. A clear limitation of the present exercise is the fact that, whereas the simulated climate response may be forcing dependent or not, as we wish to study, it is definitely model dependent. We review in conclusion the LMD GCM specificities that may affect some of our results.

2. Model description

a. Atmospheric model

We have used the low-resolution version of our atmospheric GCM coupled to a slab ocean model. The same model was used at the same resolution to study the climate response to a CO_2 doubling, the corresponding experiments being described in Le Treut et al. (1994).

The first version of the LMD GCM was described by Sadourny and Laval (1984). Although it has evolved throughout time, some basic features have remained the same. In particular, the dynamical part is written in finite differences using an Arakawa C grid, regular in sine of the latitude and in longitude. The resolution used for the experiments described below is 48 points in longitude, 36 points in sine of the latitude, and 11 levels. The standard resolutions of the LMD GCM are higher ($64 \times 50 \times 11$ and $96 \times 72 \times 15$ points). The use of this low resolution may affect the detailed partitioning of the climate response to aerosol forcing into a regional, hemispheric, or global component, as discussed below, in particular because energy and water transport by the eddies is underestimated at these low resolutions. But we believe that our results are meaningful if we restrict ourselves to a qualitative and exploratory interpretation of their implications.

The version of the model used for the experiments presented in this paper, called Cycle 4, is described in Le Treut et al. (1994). It contains a rather comprehensive physical package. The radiation scheme is the same as used in the European Centre for Medium-Range Weather Forecasts model: the solar part is a refined version of the scheme developed by Fouquart and Bonnel (1980), and the terrestrial component is due to Morcrette (1991). The solar radiation scheme distinguishes two spectral bands. The longwave radiation scheme includes six spectral bands. Condensation is parameterized separately for convective and nonconvective clouds. Convection is parameterized using in sequence a moist adiabatic adjustment and a modified version of the Kuo (1965) algorithm. A prognostic equation for cloud water is included (Le Treut and Li 1991), in which the sources and sinks of cloud-condensed water are parameterized and large-scale advection of cloud water is explicitly taken into account. The boundary layer is parameterized using a diffusive equation where the mixing coefficients depend on a prescribed length scale and a diagnostic determination of the turbulent kinetic energy. The surface conditions over land are treated using a simple bucket parameterization for moisture and a single layer for heat and moisture. This corresponds to the fact that the diurnal cycle was neglected in the present version of the model. Neglecting the diurnal cycle will prevent us from diagnosing some of the possible consequences of the aerosol loading, such as the modifications of the diurnal temperature range. This hypothesis was made to ensure the consistency of our experiments with former model scenarios. The diurnal cycle was included in the study of Boucher and Anderson (1995), and did not lead to a very different estimate of the daily averaged direct aerosol forcing.

b. Cloud representation and aerosol effects

The greenhouse forcing associated with a doubling of CO_2 concentration has been estimated for a range of climate radiative models by Cess et al. (1993). Results from the Morcrette (1991) model remain within the range of other radiative models, although the predicted forcing is slightly smaller than for other models (3.3 W m^{-2} at the tropopause, to be compared with the average value of 4.0 W m^{-2}, taking into account a range of 34% dispersion).

To predict the direct aerosol forcing, for example between present-day and preindustrial conditions, is a more difficult task. It requires the knowledge of 1) preindustrial and present-day distributions of the different aerosol types, 2) prediction of their optical properties, and 3) adequate treatment of the radiative transfer equation for a small perturbation as caused by a thin aerosol layer (Charlson et al. 1992). This direct effect has been represented under the simple form of a surface albedo

perturbation by Mitchell et al. (1995b) and Roeckner et al. (1995) to estimate its impact in transient climate scenarios using coupled ocean–atmosphere models. Such transient scenarios have also been carried out by Haywood et al. (1997). The same direct effect has been also considered more comprehensively in the experiments of Taylor and Penner (1994) where the equilibrium climate changes in response to perturbations of the greenhouse gases and sulfate aerosols, from the preindustrial epoch to the present one, were considered.

In our experiments, the sulfate aerosol concentrations are taken from the chemical transport MOGUNTIA model (Langner and Rodhe 1991; Langner et al. 1992). Aerosol optical properties are computed using standard Mie theory. We assumed the aerosol composition was ammonium sulfate and used a lognormal distribution with dry geometric volume mean diameter of 0.30 μm and geometric standard deviation of 2.0. This corresponds to the ''aerosol base case'' described in Boucher and Anderson (1995).

A physical and consistent treatment of the aerosol indirect effect requires more modifications in the model. In the present experiments we have modified the treatment of the precipitation process to include a representation of warm cloud microphysics. This is necessary to handle in a physical and consistent manner the aerosol indirect effects. This can be done explicitly in the LMD GCM because precipitation is one of the terms entering the cloud water budget equation (Le Treut and Li 1991; Le Treut et al. 1994). These modifications are described in details in Boucher et al. (1995). We summarize here the main features of the scheme and its modification. The cloud water budget equation applies to both convective and nonconvective clouds, as well as to ice and liquid phase clouds. Including the convective source of condensed water means that we take into account the strong water detrainment occurring in convective towers. As mentioned above, however, convection in the model is treated in a simplified manner. We may expect the associated detrainment to be both too intense and too low, compared to the one that would occur using a mass-flux convection scheme. Stratiform condensation is represented using a simple statistical approach, which states that water within a grid box has a distribution of a specified width (Le Treut and Li 1991). This enables the formation of fractional cloudiness in full consistency with the condensation process (and implicitly also with the cloud droplet evaporation process). The sink of cloud water is cloud evaporation and precipitation. For the latter process, two different laws are used for ice and liquid phases, respectively. Clouds are supposed to be composed of crystals when colder than -15°C and of water droplets when warmer than 0°C. A linear transition is used between those two limiting temperatures. Ice precipitation is parameterized using the sedimentation formulation of Heymsfield and Donner (1990). In the present model the precipitation of water clouds is parameterized in a complex manner, following Boucher et al. (1995). The autoconversion of cloud droplets into raindrops is treated through a parameterization depending on the mean droplet size, which in turn depends on the cloud water amount and the number concentration of CCN. The latter parameter is derived from the sulfate aerosol mass by a simple relationship as discussed in Boucher and Lohmann (1995). There are two ways in which this may affect the cloud optical depth and, hence, the earth's radiative budget. First, cloud droplet number tends to increase and cloud droplet effective radius tends to decrease with increasing CCN concentrations, which leads to brighter clouds. Then, cloud water content also tends to increase with increasing CCN concentrations, because smaller droplets precipitate less efficiently (Fouquart and Isaka 1992), which also increases cloud optical depth.

The aerosol radiative effects used here must be taken as crude estimates only, and the aerosol indirect effect is probably an overestimate as the inclusion of the explicit microphysics tends to increase low cloudiness above realistic levels. The emphasis of the present paper is on the response of the climate system to a forcing that is different in nature and distribution from the greenhouse forcing, and qualitative aspects of this response only will be discussed. It is important to note from this point of view that, as emphasized later, the largest part of the aerosol forcing in our experiments is associated with the indirect effect on warm cloud microphysics.

c. Slab ocean model

The atmospheric model is coupled with a slab ocean model. The uniform depth of the slab is set to 50 m. As already discussed in Le Treut et al. (1994), this depth does not affect the equilibrium of the model. Sea ice is supposed to occur whenever the temperature drops below -2°C. The divergence of the ocean horizontal energy transport is diagnosed as the mean surface energy flux at the atmosphere–ocean interface from an earlier atmospheric experiment using prescribed sea surface temperature. This uncoupled atmospheric experiment is run for 10 yr and uses the same CO_2 and aerosol parameters as the control scenario. This ocean transport remains unchanged throughout the various scenarios. As the average value of the surface fluxes over the oceans in the uncoupled atmospheric experiments is never exactly equal to zero, this diagnostics of the ocean transport also contains a flux correction component. But, as detailed in Le Treut et al. (1994), this simple flux correction does not prevent the coupled scenario from drifting away slightly from the control conditions. In principle, using a slab ocean with prescribed oceanic transport amounts to using a simple perturbation method, the perturbation of the surface energy fluxes between a sensitivity experiment and the control case being immediately translated into a temperature change. But, due to the slight drift of the control simulation, and as de-

scribed in section 4, the choice of the control conditions does affect the model sensitivity, and one must be correspondingly cautious in interpreting the model results.

3. Design of the experiments

As noted above, the present model was already used for sensitivity experiments to changes in the solar constant (Nesmes-Ribes et al. 1993), CO_2 doubling (Le Treut et al. 1994), and ozone perturbation (Chalita et al. 1996). In those earlier experiments the warm cloud precipitation was treated in a simplified manner, using the Sundqvist (1978) formula, or an even simpler threshold approach (Le Treut and Li 1991). New experiments have been run for the present paper, and we describe them in more detail.

1) The first experiment corresponds to present climatic conditions. It may be considered as a control case because these are the conditions in which the ocean transport has been diagnosed. It is hereafter called HCHA (high CO_2 high aerosol). We use 345 ppm for the present CO_2 concentration and present sulfate concentrations from the MOGUNTIA model, as described above.
2) A greenhouse experiment, hereafter called LCHA (low CO_2 high aerosol), where the aerosol conditions are kept to the present conditions, but the CO_2 concentration is set to its preindustrial value: 275 ppm.
3) An aerosol experiment, hereafter called HCLA (high CO_2 low aerosol), in which the CO_2 concentration is kept to the present conditions but where preindustrial aerosol distributions are used for both the radiative and precipitation schemes (i.e., for both the direct and the indirect aerosol effects).
4) A direct aerosol experiment, hereafter called HCLA-D, in which the CO_2 concentration is kept to its present value, but where the indirect aerosol effect is determined by using the preindustrial aerosol distribution. The present aerosol distribution remains used in the direct effect only. This experiment is only briefly discussed in the present paper, as the corresponding forcing is weak.
5) An experiment hereafter called LCLA (low CO_2 low aerosol), where CO_2 and aerosol concentrations both correspond to the preindustrial period.

In all experiments, the atmospheric concentration in sulfate aerosols is established from the MOGUNTIA model (Langner and Rodhe 1991; Langner et al. 1992). Another set of experiments was carried out using the ocean transport diagnosed from preindustrial rather than present forcing conditions. Some of the corresponding results are alluded to in section 4.

The forcings—always computed at the top of the atmosphere—associated with the scenarios LCHA, HCLA-D, and HCLA are displayed in Fig. 1. The greenhouse forcing is diagnosed through off-line radiative calculations. Its global average at the top of the atmosphere is 0.56 W m^{-2}. The value at the tropopause, more relevant to estimating the climatic impact of the greenhouse forcing, is twice as large: 1.06 W m^{-2}. This estimation is only an approximation because of the difficulty in defining the tropopause unambiguously. However we have tested the sensitivity of this value to slight changes in the position of the tropopause and the related incertitude is weak (around 0.05 W m^{-2}).

The direct and indirect aerosol forcings are diagnosed in a separate experiment by computing and substracting at each time step the radiative fluxes at the top of the atmosphere with industrial and preindustrial aerosol concentrations. Their global averages are, respectively, -0.26 W m^{-2} for the direct forcing and -0.81 W m^{-2} for the indirect forcing. Those values are consistent with those of Boucher and Anderson (1995) and Boucher and Lohmann (1995), in which these aerosol effects and their parameterization in our GCM are described in more detail. In the case of the aerosol forcing, as shown by Fig. 1, estimates at the top of the atmosphere or at the tropopause give similar results.

We can note however that our off-line calculations of the aerosol effect do not include any change in cloud liquid water content and therefore provide a conservative estimate of the aerosol indirect effect. This indirect effect contains in fact two parts: a change in cloud droplet concentration, which we consider as is usually done as part of the climatic forcing, and a change in cloud water content, which we consider as a feedback process. This distinction is a matter of definition and another estimate of the indirect forcing, which includes part of the cloud feedbacks, can also be obtained by making differences of the mean radiative fluxes at the top of the atmosphere during the first year of the various experiments (i.e., before the system begins to evolve drastically). The geographical distributions are affected by noise, because of the variability of the atmospheric circulation, which is not the same in the different simulations, but are consistent with the results shown here, with a slightly higher global value, which account for the liquid water feedback. In any case, our forcing estimates are indicative only, with a possible tendency to overestimate the indirect effect—the low cloudiness tends to be too important in the version of the model including cloud microphysics, as noted in Boucher et al. (1995) and as stated above—and to underestimate the direct effect.

To summarize, in each of our sensitivity experiments, the radiative forcing is diagnosed through off-line radiative calculations by difference of the radiative balance between the perturbed and unperturbed conditions, at each level of the model, as displayed in Fig. 2. The global forcing taken into account to evaluate the global climate sensitivity in the next paragraph is somewhat arbitrarily defined as the maximum of the zonally averaged vertical profile. The four cases shown in Fig. 2 show how different the structure of the forcing may be depending on a particular radiative perturbation. While

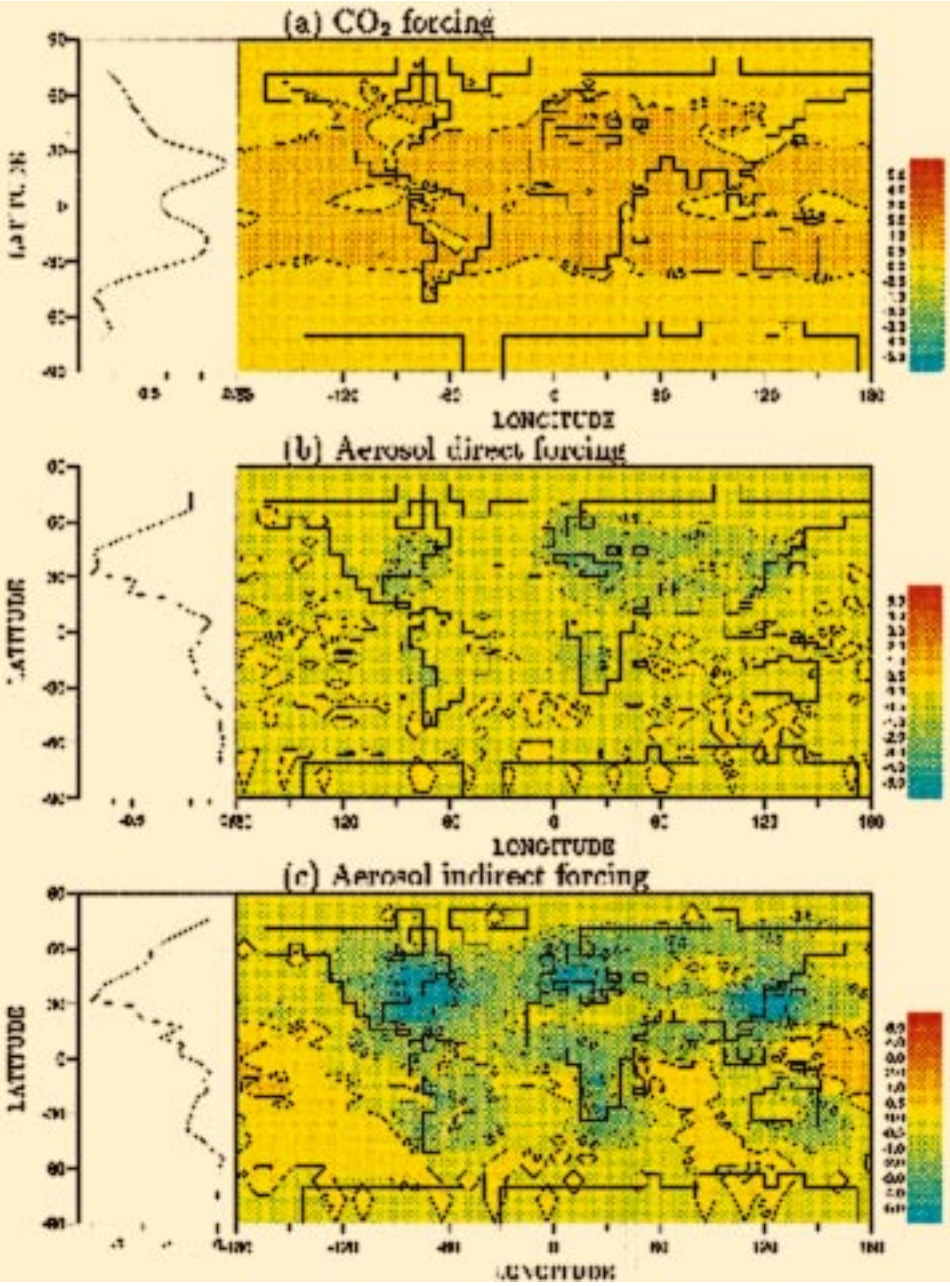

FIG. 1. Climate forcings (W m^{-2}) due to (a) the CO_2 greenhouse effect, (b) the aerosol direct effect, and (c) the aerosol indirect effect.

in the aerosol case the main dependency is in latitude with a very small vertical divergence of the flux—a feature that also appears in the solar forcing experiment, but less pronounced—the greenhouse effect is neutral at the tropopause, with a cooling tendency above and a warming tendency below. This means that a solar perturbation such as the aerosols acts mainly through changes in the ground temperature, and the corresponding feedback effects, involving the indirect microphysical response, will also largely be triggered by the change in ground temperature. On the contrary the direct heating of the atmosphere may be more important in the greenhouse scenarios.

4. Results

All experiments are carried out for 20 yr. The time evolution of the globally averaged temperature for the different experiments is shown in Fig. 3. As mentioned earlier, our simple flux correction coupling does not pre-

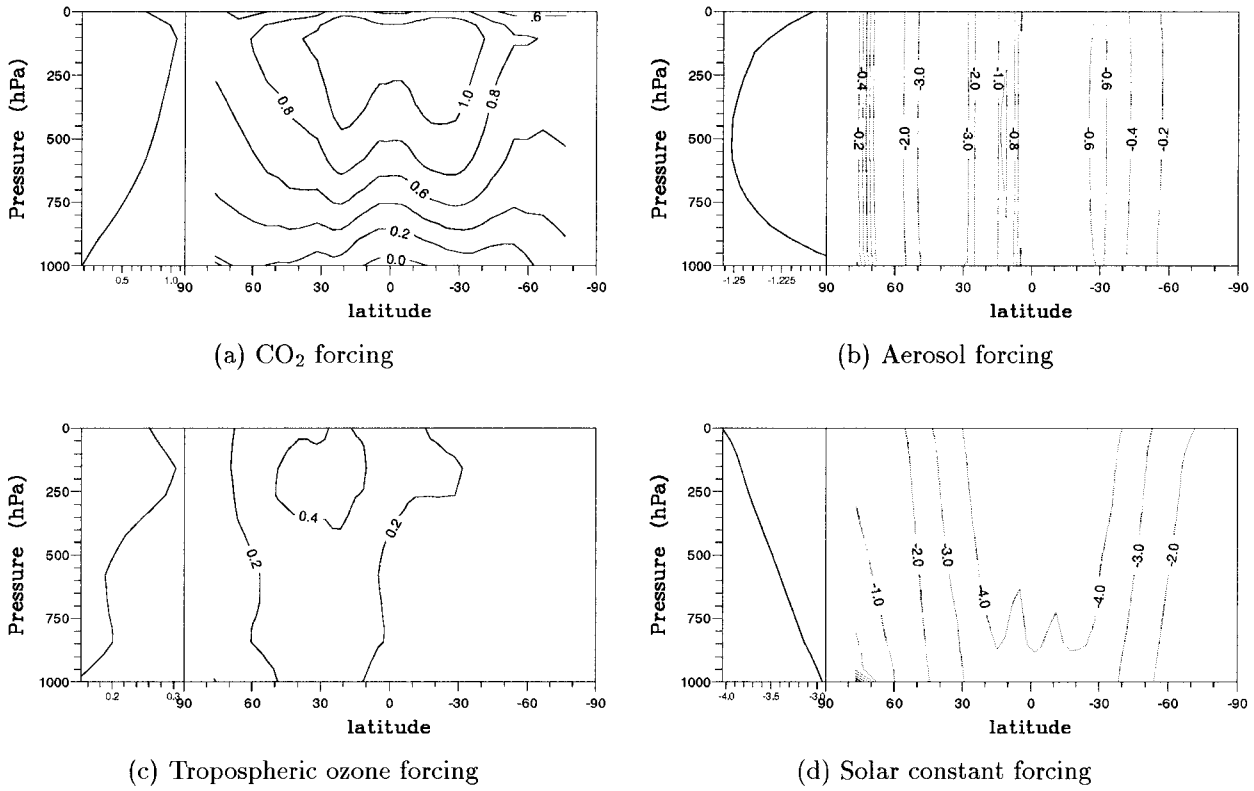

FIG. 2. Zonally averaged vertical profiles of the different radiative forcings (W m^{-2}): (a) CO_2 forcing, (b) aerosol indirect forcing, (c) tropospheric ozone forcing, and (d) solar constant forcing.

vent the control scenario from drifting slightly. From now on, the averages for all experiments are taken over the last 10 yr. For convenience we represent the results as differences between the control (HCHA) and a given experiment. In that way, the greenhouse effect appears as a warming, and the aerosol effects as a cooling.

We have gathered a number of global results concerning experiments HCHA, LCHA, HCLA, and LCLA in Table 1. These experiments illustrate the very large dependence of the model sensitivity to the mean atmospheric temperature. The aerosol effect can be detected using the difference between HCHA and HCLA, which gives a cooling of 1.57 K, or as the difference between LCHA and LCLA, which gives a cooling of 2.86 K. Similarly the greenhouse effect of the CO_2 can be diagnosed as the difference between LCHA and HCHA, which gives a warming of 2.81 K, or between the experiments LCLA and HCLA, which gives a warming of 1.51 K. This illustrates the fact, which is general in our simulations, that a cooler control case gives a higher model sensitivity.

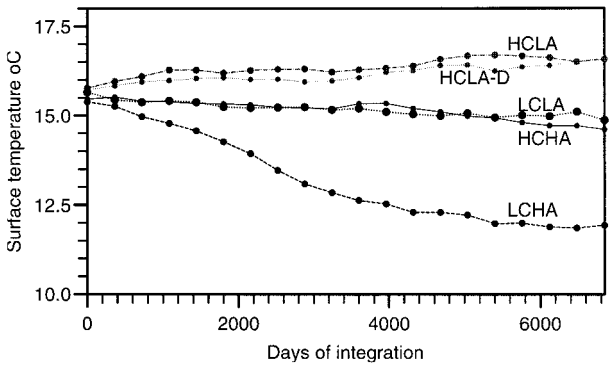

FIG. 3. Temporal evolution of the globally averaged surface temperature (°C) in the various experiments.

To further demonstrate this point we have gathered in the upper panel of Fig. 4 all the results of the different scenarios made with the LMD4 model version, which differ only through their radiative forcing and details of the precipitation term in the cloud schemes. All the results are plotted as a difference between a perturbation and a control, where the conditions corresponding to the present climate are always chosen as the control: this simple criterion decides whether the perturbation is positive or negative. The results tend to place themselves on a curve, a feature that shows clearly that, for our model at least, the notion of model sensitivity is a relevant one and is only slightly dependent on the nature of the radiative forcing. Incidentally, this gives credit to the idea of characterizing greenhouse gases separately through their warming potential.

The lower panel of Fig. 4 adds to the temperature

TABLE 1. Climate statistics for the different experiments. The different quantities are global averages for the last 10 yr of the different simulations.

Experiment	HCHA	LCHA	HCLA	LCLA
CO_2 (ppm)	345	275	345	275
Aerosol level	Present	Present	Preindustrial	Preindustrial
Surface temp (°C)	14.97	12.16	16.53	15.02
Water vapor (kg m^{-2})	28.58	23.47	31.78	29.22
Cloud water (g m^{-2})	66.44	60.04	68.24	65.38
Precipitation rate (mm day^{-1})	3.37	3.26	3.47	3.41
Evaporation rate (mm day^{-1})	3.37	3.26	3.47	3.41
Cloud cover (%)	70	70	69	70
Ground albedo	0.13	0.15	0.13	0.14
Cloud radiative forcing (W m^{-2})				
longwave	38.07	35.14	39.12	38.72
shortwave	−54.66	−52.56	−55.19	−53.81

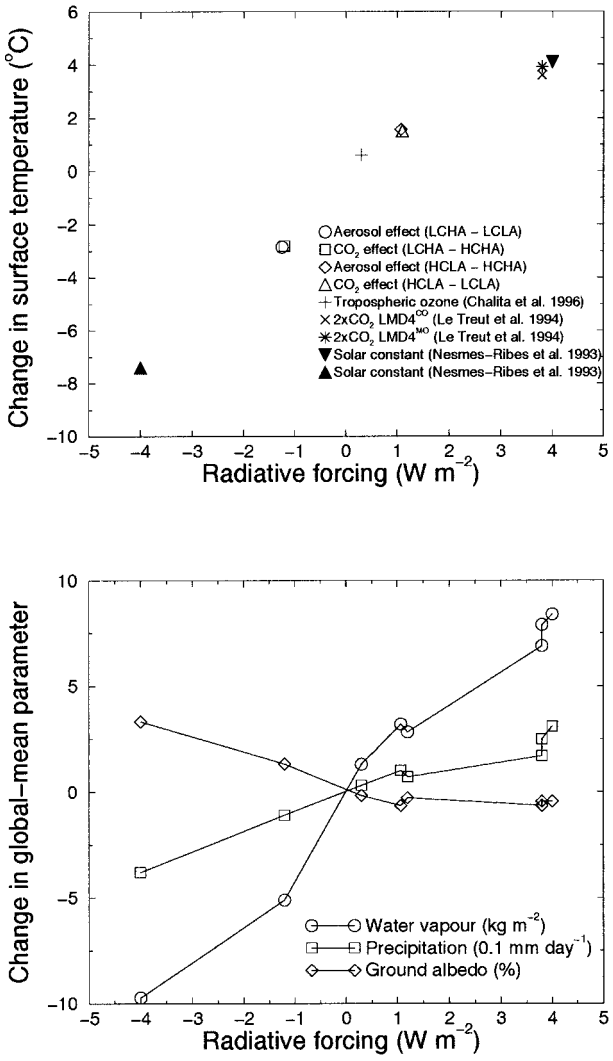

FIG. 4. (upper panel) Change of global mean temperature (°C) in response to various climate forcings. (lower panel) Change of global mean climatic parameters (precipitable water, precipitation, ground albedo) in response to various climate forcings.

response the behavior of a few parameters. It shows a similar type of behavior, with a partial independence of the response from the forcing, although less pronounced. The important feature to be noted as far as the temperature response is concerned is the higher sensitivity of the model in colder climate conditions. The respective impact of the aerosol and greenhouse effects therefore depends on the reference climatic state, and we cannot expect them to combine linearly.

We can note, from Table 1, that the LCLA experiment leads to a very close temperature as in HCHA, which means a near cancellation of both greenhouse and aerosol effects on the average. In view of the exploratory and qualitative character of our experiments no effort was made to include at this stage other atmospheric trace gases (e.g., CH_4, CFCs, or tropospheric O_3, the latter being the subject of separate experiments not reported here), or other aerosol types (e.g., industrial black carbon and organic aerosols, or biomass burning aerosols). The near cancellation of the greenhouse and aerosol effects in our experiments therefore appears purely coincidental, but it offers a nice illustration of the nonlinearities of the climate response, which we try to exploit by analyzing the greenhouse and aerosol effects in similar conditions, and comparing the associated feedbacks in simulations where the temperature changes have a similar magnitude.

In particular we use the LCLA and HCLA experiments to diagnose the greenhouse effect, and the experiments HCLA and HCHA to diagnose the aerosol effect. In this case we compare a warm experiment (HCLA) to two experiments corresponding in global average temperature to present climatic conditions (LCLA or HCHA). The results of Table 1 show that the temperature changes associated with the greenhouse and aerosol effects are then + or −1.5 K respectively. We could have used alternatively HCHA and LCHA to diagnose the greenhouse effect and LCHA and LCLA to diagnose the aerosol impact. We would then make use of a colder reference (LCHA) and the resulting sensitivity would be much higher (+ or −2.8 K, making use again of the results gathered in Table 1).

The results of Table 1 also show that in this low-resolution version of the LMD GCM the hydrological cycle is very active, with high evaporation and precipitation values, and a large cloud cover. We may note however that the LMD GCM makes use of a random overlapping of partially covered cloud layers, a feature that increases the total cloud cover. Also, the mean cloud radiative forcing has the correct order of magnitude.

A global estimation of the various feedbacks can be deduced from Table 1. The cloud water and water vapor changes follow roughly the mean temperature variations, but we may note that the experiment with more aerosols (HCHA) has a higher cloud water and a lower water vapor amount, for temperature conditions similar to those of LCLA. These results are consistent with the expected impact of the aerosol forcing. The total cloud cover changes little, although the vertical distribution of cloudiness changes as emphasized later.

The mean changes in surface temperature (HCLA − LCLA, HCHA − HCLA, HCHA − LCLA) are shown in Fig. 5. The spatial structure of the response to this greenhouse forcing is very similar to the response to a CO_2 doubling described in Le Treut et al. (1994). The aerosol response is also surprisingly similar to this large-scale greenhouse response, but with opposite sign. It shows in particular the same pattern of polar amplification. The response is extremal near Antarctica, a region where the aerosol forcing is negligible. The larger response over the continents is also similar in the two cases (greenhouse forcing and aerosol forcing), in spite of very different forcing conditions. In the aerosol case, the forcing is indeed larger over the continents. But the greenhouse forcing has similar values over the continents and oceans, and the simulated amplification of the response over the continents is due to processes internal to the climate system. The existence of a large-scale response, uncorrelated spatially with the forcing, is therefore an important characteristic of our simulations. Similar results have been obtained with other model simulations, such as those reported by Taylor and Penner (1994). We are conscious however that it may be very model dependent. For example, the present version of our GCM seems to be very sensitive to changes in sea-ice cover (Le Treut et al. 1994), a feature that may increase the Southern Hemisphere response to aerosol forcing.

The latitude–altitude distributions shown in Fig. 6 confirm that the structure of the warming (or cooling) patterns in response to the two forcings is similar, in spite of quantitative differences concerning the asymmetry between the two hemispheres, and the stratospheric cooling (or warming). In the case where the aerosol and greenhouse forcings are combined we nevertheless obtain a warming hemisphere and a cooling one. In both hemispheres the tendency for an amplification of the response in polar regions is maintained. Everything happens as if both hemispheres were organized with a large-scale pattern somewhat independent of the forcing, with a distinction between an ''aerosol hemisphere'' (the northern one) and a ''greenhouse hemisphere'' (the southern one).

These results support the idea that the climate system, or at least our model representation of it, has a large-scale response driven by atmospheric or surface feedbacks. These feedbacks may have different natures: changes in the horizontal transport of water and energy as well as changes in the radiative components of the climate system. As we study equilibrium scenarios, there is however a compensation between mean changes in the divergence of horizontal energy transport and vertical heat fluxes. In Le Treut et al. (1994) we had analyzed for our model the correspondence between simulated changes of the cloud and water distributions associated with a CO_2 doubling, and the related changes in radiative fluxes, and shown that a large part of the surface temperature changes could be attributed to these radiative changes. For all these reasons, the changes in the mean distribution of temperature, water vapor, and cloud properties constitute a first qualitative approach of the internal feedback effects at work in our simulations.

The change in water vapor is shown in Fig. 7a for the greenhouse forcing experiment (HCLA − LCLA) and in Fig. 7b for the aerosol experiment (HCHA − HCLA). Although there are differences—the aerosol response is more concentrated and more intense at low latitudes, and the asymmetry with respect to the equator is opposite—the most striking feature is that in both cases the maximum response is near the equator and not in the forcing regions for the aerosol case. We then show the cloud liquid water difference, again between experiments HCLA and LCLA (Fig. 8a) and HCHA and HCLA (Fig. 8b). The structure is qualitatively similar to that described for previous CO_2 doubling experiments (Le Treut et al. 1994; Mitchell et al. 1995a). In association with a global warming or cooling, the cloud water tends to increase or decrease, respectively, in the intertropical areas, where a lower (higher) intensity of the Hadley cell is more than compensated for by the warmer and moister (cooler and drier) air in the low converging branch of the circulation. Cloud water is also increased (decreased) near 60°N and 60°S, in response to latitudinal shifts of the transition between predominantly solid and predominantly liquid low clouds. This pattern may be explained through thermodynamical processes (including local turbulence and convection) probably because in these scenarios the perturbation of the atmospheric circulation has only a higher-order effect.

The same explanation does not hold for more extreme scenarios like the drastic simulation of the last glacial maximum, described by Ramstein et al. (1998). The specific impact of the aerosols is only visible in the subtropical area where an increase in the aerosol concentration leads to an increase in the cloud water content, which is more pronounced and more extended than the corresponding decrease associated with the CO_2

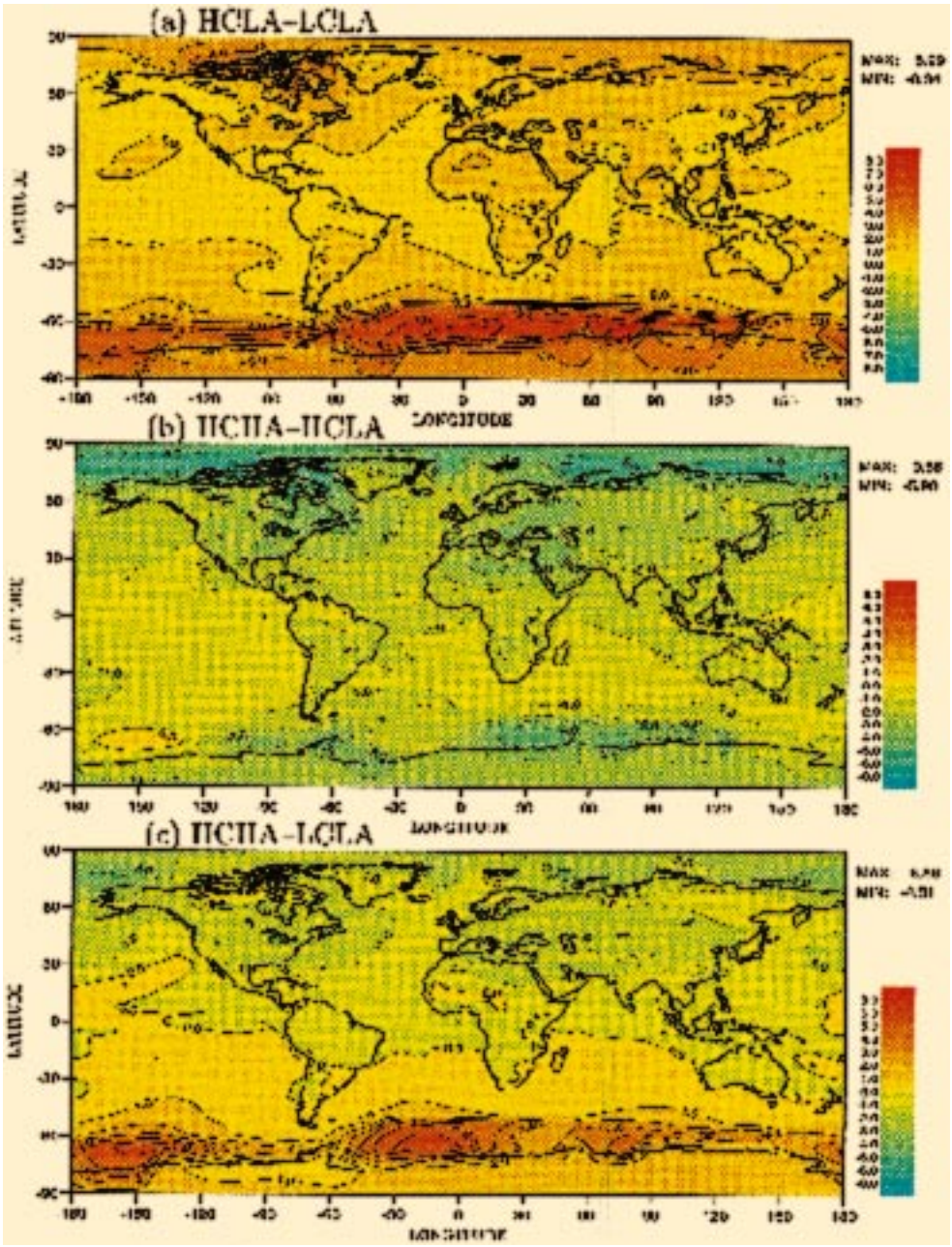

FIG. 5. Annual average surface temperature change (°C) in response to (a) the CO_2 forcing (HCLA − LCLA), (b) the aerosol forcing (HCHA − HCLA), and (c) the combined aerosol and CO_2 forcings (HCHA − LCLA).

warming. But this additional effect due to aerosols, which is important locally, does not modify the global structure of the cloud water response. If we extend this diagnostics to cloud fraction differences (Figs. 9a and 9b), we may note the same general symmetry in the two responses to the CO_2 and aerosol forcings, except at 60°N near the ground. In that case the structure of the model response is more complex than for cloud water, because of a general tendency to have less (resp. more) low cloudiness and more (resp. less) high cloudness associated with a global warming (resp. cooling). The symmetry of this rather complex structure of the cloud cover response is a striking illustration of the global organization of the feedback amplification of any climate change. The results of this section also suggest that atmospheric feedbacks may constitute a very strong feature linking the two hemispheres and may, for example, constitute a plausible mechanism to explain the

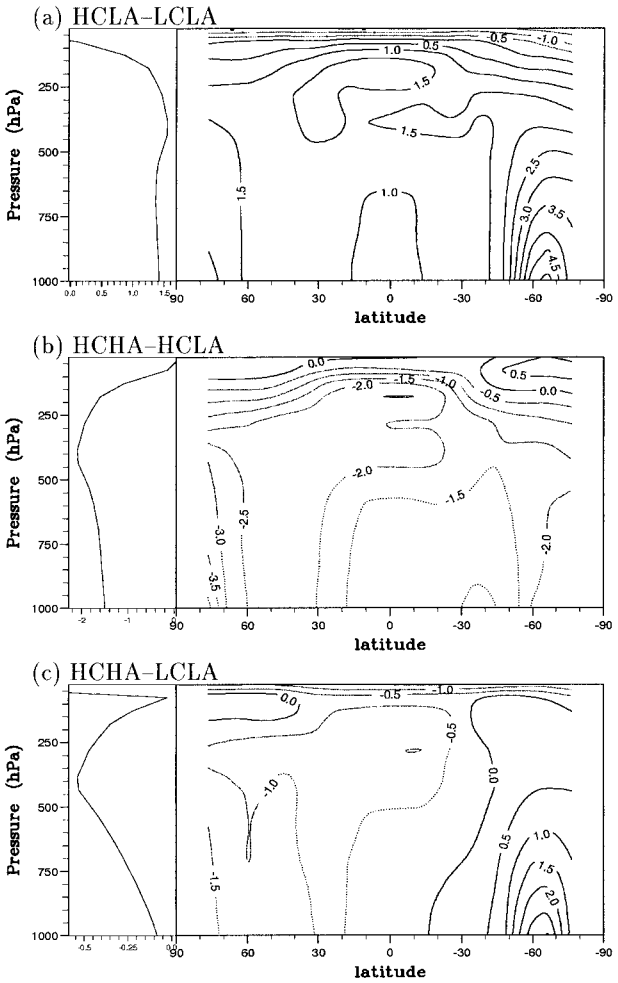

FIG. 6. Annually and zonally averaged temperature changes (°C) in response to (a) the greenhouse forcing (HCLA − LCLA), (b) the aerosol forcing (HCHA − HCLA), and (c) the combined greenhouse and aerosol forcings (HCHA − LCLA).

synchronism of the glaciations between the two hemispheres (M. Bender et al. 1996, unpublished manuscript).

5. Conclusions

Internal feedback processes within the climate system have a major impact on the climate response to radiative perturbations. These feedback effects are probably very model dependent, but they strongly control the amplitude of the simulated response to anthropogenic forcings such as the increase in greenhouse gases or aerosol concentration. These feedback effects may also control, to a large extent, the main geographical patterns of the climate change manifestations. To investigate this point, we have compared the response of the LMD GCM to perturbations of different natures: CO_2 increase, and aerosol direct and indirect effects since the beginning of the industrial period. Unlike most other experiments

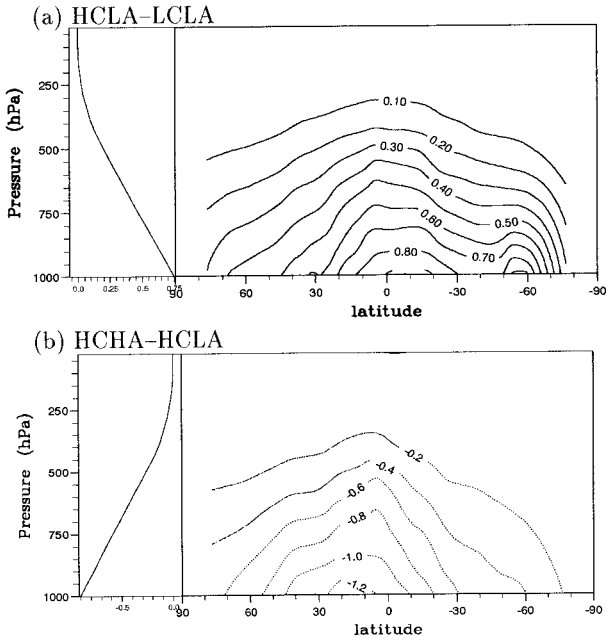

FIG. 7. Zonally averaged change in specific humidity (g kg^{-1}) in response to (a) the greenhouse forcing (HCLA − LCLA) and (b) the aerosol forcing (HCHA − HCLA).

so far, we have taken into account explicitly most of the relevant physical processes and, in particular, the microphysics of low clouds. The role of ice microphysics, however, is still crudely represented and should be the focus of further studies. The ocean is represented

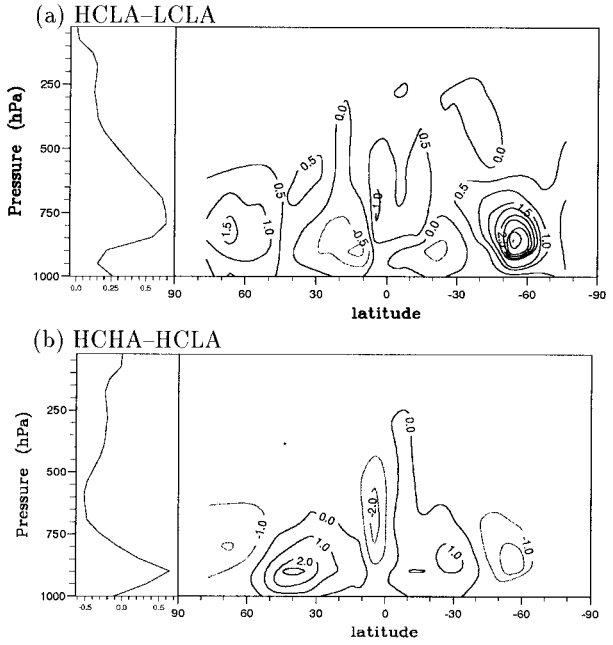

FIG. 8. Zonally averaged change in cloud water content (mg kg^{-1}) in response to (a) the greenhouse forcing (HCLA − LCLA) and (b) the aerosol forcing (HCHA − HCLA).

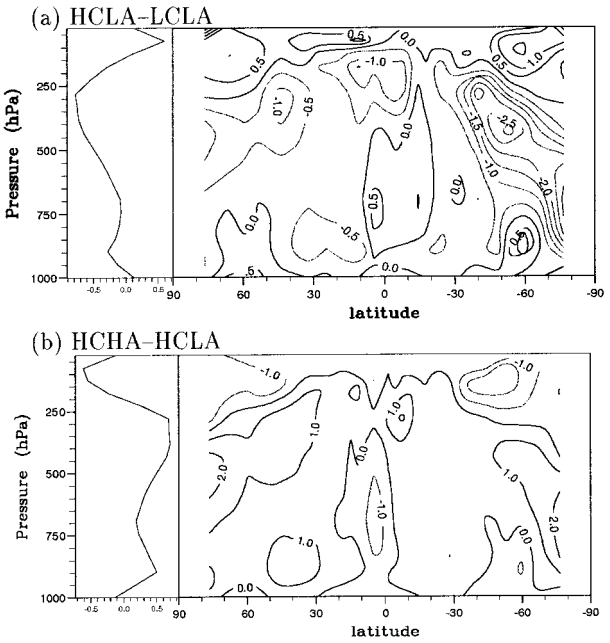

FIG. 9. Zonally averaged change in cloud cover (%) in response to (a) the greenhouse forcing (HCLA − LCLA) and (b) the aerosol forcing (HCHA − HCLA).

by a simple slab of 50 m, with prescribed oceanic energy transport. As a consequence, the control of the climate response is entirely the result of surface and atmospheric processes, with no participation of the internal oceanic processes. Our model also lacks a sufficient resolution in the stratosphere, a zone where a crucial differentiation between solar and longwave perturbations may occur. Finally, another important reason to interpret our results only in a qualitative manner is the simplified design of the experiments and the nonlinearity of the involved processes.

In spite of these reservations, the most striking feature of our results is that the response to the two types of forcings shows partial similarities at the synoptic scale and presents in all cases a poleward amplification. This remains true even in the case where the combination of the two forcings split the model response in a northern ''aerosol hemisphere'' and a southern ''greenhouse hemisphere.'' In our experiments the major cloud feedback processes are explicitly described and the spatial structure of their effect in response to the different forcings also presents a striking symmetry between warming and cooling scenarios. This has several implications. First, it may be more difficult than anticipated to sort out the climate responses to different anthropogenic and natural forcings over the past century by using the observed temperature records, as is already apparent from the results of Taylor and Penner (1994) and Santer et al. (1995). The local simulated response may be very model dependent and may be the response to a set of partially compensating forcings, organized at the global scale through imperfectly known processes. The LMD GCM response, in particular, although it is consistent with the finding of other models (Meehl et al. 1996), may be distorted by a too large sea-ice feedback or a too close association of tropical cloudiness with the occurrence of convective events.

In spite of this qualitative correspondence between the response to aerosol and greenhouse forcings, the asymmetry between the two hemispheres is maintained, and even accentuated, when we combine these two forcings. The temperature redistribution through atmospheric processes is then apparently active in each hemisphere separately. As noted by Santer et al. (1995), the asymmetry between the two hemispheres may therefore constitute the first and so far only firm effect on which to base a strategy for climate change detection. But such global indices will be useful only if our knowledge of the radiative forcing exerted on the earth's system is also improved. A better estimation of the aerosol direct and indirect effects and a better physical consistency of the models are the two prior requirements for that purpose.

Acknowledgments. We thank Pr. Henning Rodhe and Ulf Hansson for providing the sulfate aerosol data. Computer time for numerical experiments was provided by IDRIS (Institut de Développement et des Ressources en Informatique Scientifique). This work was partly supported by the Environmental Programme of the European Commission and the PNEDC (French National Climate Dynamics Programme).

REFERENCES

Boucher, O., and T. L. Anderson, 1995: GCM assessment of the sensitivity of direct climate forcing by anthropogenic sulfate aerosols to aerosol size and chemistry. *J. Geophys. Res.,* **100,** 26 117–26 134.

——, and U. Lohmann, 1995: The sulfate–CCN–cloud albedo effect: A sensitivity study using two general circulation models. *Tellus,* **47B,** 281–300.

——, H. Le Treut, and M. B. Baker, 1995: Precipitation and radiation modeling in a GCM: Introduction of cloud microphysics. *J. Geophys. Res.,* **100,** 16 395–16 414.

Cess, R. D., and Coauthors, 1993: Uncertainties in carbon dioxide radiative forcing in atmospheric general circulation models. *Science,* **262,** 1252–1255.

Chalita, S., D. A. Hauglustaine, H. Le Treut, and J.-F. Müller, 1996: Radiative forcing due to increased tropospheric ozone concentrations. *Atmos. Environ.,* **30,** 1641–1646.

Charlson, R. J., J. E. Lovelock, M. O. Andreae, and S. G. Warren, 1987: Oceanic phytoplankton, atmospheric sulphur, cloud albedo, and climate. *Nature,* **326,** 655–661.

——, S. E. Schwartz, J. M. Hales, R. D. Cess, J. A. Coakley, J. E. Hansen, and D. J. Hofmann, 1992: Climate forcing by anthropogenic aerosols. *Science,* **255,** 423–430.

Fouquart, Y., and B. Bonnel, 1980: Computations of solar heating of the earth's atmosphere: A new parameterization. *Beitr. Phys. Atmos.,* **53,** 35–62.

——, and H. Isaka, 1992: Sulfur emission, CCN, clouds and climate: A review. *Ann. Geophys.,* **10,** 462–471.

Haywood, J. M., R. J. Stouffer, R. T. Wetherald, S. Manabe, and V. Ramaswamy, 1997: Transient response of a coupled model to

estimated changes in greenhouse gas and sulfate concentrations. *Geophys. Res. Lett.,* **24,** 1335–1338.

Heymsfield, A. J., and L. J. Donner, 1990: A scheme for parameterizing ice-cloud water content in general circulation models. *J. Atmos. Sci.,* **47,** 1865–1877.

Kuo, H. L., 1965: On formation and intensification of tropical cyclones through latent heat release by cumulus convection. *J. Atmos. Sci.,* **22,** 40–63.

Langner, J., and H. Rodhe, 1991: A global three-dimensional model of the tropospheric sulfur cycle. *J. Atmos. Chem.,* **13,** 225–263.

——, ——, P. J. Crutzen, and P. Zimmermann, 1992: Anthropogenic influence of the distribution of tropospheric sulphate aerosol. *Nature,* **359,** 712–716.

Le Treut, H., and Z.-X. Li, 1991: The sensitivity of an atmospheric general circulation model to prescribed SST changes: Feedback effects associated with the simulation of cloud optical properties. *Climate Dyn.,* **5,** 175–187.

——, ——, and M. Forichon, 1994: Sensitivity of the LMD general circulation model to greenhouse forcing associated with two different cloud water parameterizations. *J. Climate,* **7,** 1827–1841.

Meehl, G. A., W. M. Washington, D. J. Erickson III, B. P. Briegleb, and P. J. Jauman, 1996: Climate change from increased CO_2 and direct and indirect effects of sulfate aerosols. *Geophys. Res. Lett.,* **23,** 3755–3758.

Mitchell, J. F. B., R. A. Davis, W. J. Ingram, and C. A. Senior, 1995a: On surface temperature, greenhouse gases, and aerosols: Models and observations. *J. Climate,* **8,** 2364–2386.

——, T. C. Johns, J. M. Gregory, and S. F. B. Tett, 1995b: Climate response to increasing levels of greenhouse gases and sulphate aerosol. *Nature,* **376,** 501–504.

Morcrette, J.-J., 1991: Radiation and cloud radiative properties in the European Centre for Medium Range Weather Forecasts forecasting system. *J. Geophys. Res.,* **96,** 9121–9132.

Nesmes-Ribes, E., E. N. Ferreira, R. Sadourny, H. Le Treut, and Z.-X. Li, 1993: Solar dynamics and its impact on solar irradiance and the terrestrial climate. *J. Geophys. Res.,* **98,** 18 923–18 935.

Penner, J. E., and Coauthors, 1994: Quantifying and minimizing uncertainty of climate forcing by anthropogenic aerosols. *Bull. Amer. Meteor. Soc.,* **75,** 375–400.

Ramstein, G., V. Serafini, H. Le Treut, M. Forichon, and S. Joussaume, 1998: Cloud processes associated with past and future climate changes. *Climate Dyn.,* in press.

Roeckner, E., T. Siebert, and J. Feichter, 1995: Climatic response to anthropogenic sulfate forcing simulated with a general circulation model. *Aerosol Forcing of Climate,* R. Charlson and J. Heintzenberg, Eds., John Wiley and Sons, 349–362.

Sadourny, R., and K. Laval, 1984: January and July performance of the LMD general circulation model. *New Perspectives in Climate Modelling,* A. Berger and C. Nicolis, Eds., Elsevier, 173–198.

Santer, B. D., K. E. Taylor, T. M. L. Wigley, J. E. Penner, P. D. Jones, and U. Cubasch, 1995: Towards the detection and attribution of an anthropogenic effect on climate. *Climate Dyn.,* **12,** 77–100.

Sundqvist, H., 1978: A parameterization scheme for non-convective condensation including prediction of cloud water content. *Quart. J. Roy. Meteor. Soc.,* **104,** 677–690.

Taylor, K. E., and J. E. Penner, 1994: Response of the climate system to atmospheric aerosols and greenhouse gases. *Nature,* **369,** 734–737.